

DESIGN OF A LOW-SPEED ICING WIND TUNNEL FOR UAVS

J. Wallisch, R. Hann;
Norwegian University of Science and Technology
Centre for Autonomous Marine Operations
Department of Engineering Cybernetics
7034 Trondheim, Norway

Abstract

Atmospheric icing is a key challenge of the operational envelope of unmanned aerial vehicles. Especially medium-sized fixed-wing UAVs suffer from the consequences of ice accretions. Icing wind tunnels are important facilities to do experiments and gain more insight into atmospheric icing. However, the number of suitable icing wind tunnels for UAVs is low. This work describes the design of a possible icing wind tunnel specifically designed for UAV applications. The icing wind tunnel design is of the open-return type and has a dimension of 8 m x 1.5 m x 1.5 m. With the possibility to test median volume diameters of maximum 40 µm, the icing wind tunnel covers a wide range of in-cloud icing conditions. To ensure a steady run of the icing wind tunnel, a fan power of 8 kW is necessary as well as a cooling power of 20 kW. This work also contains the results of flow simulations of the icing wind tunnel. These CFD results show flow separation which needs to be taken into consideration for the next design steps.

NOMENCLATURE

Latin Symbols

A	[m ²]	area
AR	[\cdot]	area ratio
c_D	[\cdot]	drag coefficient
c_{latent}	[J/kg]	specific latent heat of fusion
c_p	[J/(kgK)]	specific heat capacity at constant pressure
c_v	[J/(kgK)]	specific heat capacity at constant volume
d	[\cdot]	differential
\dot{E}	[W]	rate of change of internal energy
\vec{g}	[m/s ²]	vector of gravity
k	[W/(mK)]	heat conductivity
L	[m]	length
m	[kg]	mass
\dot{m}	[kg/s]	water mass flow rate
Nu	[\cdot]	Nusselt number
Pr	[\cdot]	Prandtl number
\dot{Q}	[W]	heat flux
Re	[\cdot]	Reynolds number
r	[m]	radius
T	[K]	temperature
t	[s]	time
\vec{u}	[m/s]	speed vector of the droplets
\dot{V}	[m ³ /s]	volume flux
v	[m/s]	air speed
\vec{v}	[m/s]	speed vector of the air
x	[m]	coordinate in streamwise direction
z	[m]	coordinate perpendicular to streamwise direction

Greek Symbols

Δ	[\cdot]	difference
ϵ	[\cdot]	emissivity
ρ	[kg/m ³]	density

σ [W/(m²K⁴)] Stefan-Boltzmann constant

Indizes

a	ambient
air	value of the air
C	convection
d	value of the droplet
$latent$	latent heat
R	radiation
$sensible$	sensible heat
TS	value at test section
$water$	value of water

Abbreviations

CFD	computational fluid dynamics
EASA	European Union Aviation Safety Agency
LWC	[kg/m ³]
MVD	[m]
UAV	unmanned aerial vehicle

1. INTRODUCTION

Aircraft have to deal with several challenging weather conditions. Atmospheric icing is one of them. Atmospheric icing occurs when aircraft fly through clouds with supercooled liquid water droplets. Some of the water droplets will hit the aircraft and freeze. The accreted ice has several negative impacts on the aircraft performance. The lift of the wing is reduced as well as the stall angle, while the drag of the aircraft is increased [1]. Ice on the propulsion system additionally reduces the thrust of the aircraft. Therefore, the capability of an aircraft is reduced significantly by atmospheric icing. If an aircraft is operated in icing conditions, the risk of losing the aircraft is substantially increased. Hence, aircraft often have to stay grounded during icing conditions [2].

Icing is particularly dangerous for medium-sized unmanned aerial vehicles (UAV) [3]. This is because - except for the largest UAVs - UAVs are smaller in size and fly at lower speeds and altitudes compared to manned aircraft. Being smaller in size and flying at lower speeds results in lower Reynolds numbers. The ice accretion processes depend to a large degree on the Reynolds number [4]. Additionally, aircraft with lower Reynolds numbers typically accrete a larger relative amount of ice when flying through the same cloud as an aircraft with a higher Reynolds number – resulting in higher losses [5]. Therefore, UAVs need suitable ice protection systems to also operate in icing conditions. While many mature technologies for ice protection systems exist for manned aircraft, such systems are relatively new and immature on UAVs.

An important feature to increase the knowledge about atmospheric icing and to test ice protection systems are icing experiments in wind tunnels. Such a wind tunnel needs to be able to inject water droplets into the airstream and supercool them before the droplets hit the airfoil. There exist several icing wind tunnels, mainly designed for the needs of manned aircraft [6]. As UAVs operate at lower Reynolds numbers, the same icing wind tunnels can often not be used for icing experiments on UAVs. Therefore, the number of icing wind tunnels that fit the requirements of UAVs is very low. This is why there are many numerical investigations on icing on UAVs (e.g. [7],[8],[9],[10]), but just a few experimental tests(e.g. [11],[12]).

The usage of different icing wind tunnels for UAVs and manned aircraft is also based on the difficulties of scaling the results of icing experiments. For scaling, a total of 18 dimensionless numbers have to be matched to rebuild the effects of the flow field, the droplet trajectories, and the impingement and freezing of the droplets [13]. Scaling, therefore, introduces substantial challenges and is often avoided when possible.

The significant challenges of UAVs in icing conditions on one side, and the lack of suitable icing wind tunnels for UAVs on the other side, lead to the need of new icing wind tunnels specifically designed for UAVs. This is why the design of a low-speed icing wind tunnel for medium-sized fixed-wing UAVs was initiated by the Norwegian University of Science and Technology [14].

2. METHODS

2.1. The design of a wind tunnel

The design of an icing wind tunnel starts by designing a conventional wind tunnel. This study proposes a conventional open-return wind tunnel. The main components are a test section, a diffuser, a contraction, a settling area, and a fan.

The test section is the most important component of every wind tunnel because the test object is mounted in the test section and the measurements take place there as well. Therefore, the size of the test section defines which objects can be tested in the designed wind tunnel. The size of the test section also drives the overall dimensions of the wind tunnel and also the required power. Hence, the test section must be designed as large as necessary to contain the chosen test objects, but as small as possible.

A contraction nozzle is installed upstream of the test section to accelerate the flow. A 1D-analysis suggested that the flow will not separate in the contraction nozzle because the flow is accelerated. More detailed investigations with computational fluid dynamic (CFD) simulations however showed a risk of separation close to the beginning and the end of the contraction nozzle [15]. To prevent separation, the closing angle must be limited. Additionally, a nozzle contour with large radii at the beginning and end is beneficial for preventing separation, too.

The settling area is placed upstream of the contraction nozzle. The settling area contains components that increase the flow quality. These components are typically divided into honeycombs and turbulence screens. Honeycombs resemble small pipes intended to reduce turbulence. Because of their high length-to-diameter ratio, they reduce the component of the flow velocity normal to the flow direction. The turbulence screens are wires. These wires lead to pressure losses proportional to the square of the speed and therefore reduce the non-uniformities in the flow.

A diffuser is installed downstream of the test section. The flow is decelerated because of the cross-section expansion. Because of the decreasing speed, the flow in the diffuser is prone to separate. Separation in the diffuser reduces the flow quality in the test section as well. Hence, separation must be prevented. The risk of separation is reduced by choosing smaller opening angles of the diffuser. Because of the reduced velocity at the exit of the diffuser, the kinetic energy is reduced as well. This leads to a reduced pressure loss of the wind tunnel in total. The reduced kinetic energy at the exit of the diffuser is particularly important for open-return wind tunnels. This is because the kinetic energy at the exit of an open-return wind tunnel is lost completely.

2.2. Necessary fan and cooling power

Minimizing the pressure loss is important because a fan needs to compensate the overall pressure loss in the wind tunnel. By minimizing the pressure loss, the required fan power is reduced as well. Pressure losses occur at every component of the wind tunnel, mostly due to friction. A calculation of the total pressure loss of the wind tunnel can be done by summing up the pressure loss of every single component [15]. The fan does not only need to compensate for the pressure loss in the wind tunnel but also needs to force air through the wind tunnel. The volume flow

$$(1) \quad \dot{V} = vA$$

through the wind tunnel depends on the speed v in the test section and the cross-sectional area A of the test section. Therefore, a careful selection of the maximum airspeed of the tunnel is required in order to minimize the pressure loss.

To transform a conventional wind tunnel in an icing wind tunnel, two components need to be added: a spray system that injects liquid water droplets and a cooling unit.

Heat is produced during the run of the wind tunnel and needs to be removed by the cooling unit. Otherwise, the air temperature will rise rapidly [15]. During the run of an icing wind tunnel, heat is produced in three different ways [16]. First, heat is generated by the wind tunnel fan. Second, the sensible heat

$$(2) \dot{Q}_{\text{sensible}} = \dot{m}_{\text{water}} c_{p,\text{water}} \Delta T$$

needs to be removed to cool the water droplets from their initial temperature to their final temperature. The last heat term is the latent heat. The latent heat

$$(3) \dot{Q}_{\text{latent}} = \dot{m}_{\text{water}} c_{\text{latent},\text{water}}$$

is released when water freezes. Both the latent heat and the sensible heat depend on the flow rate of water

$$(4) \dot{m}_{\text{water}} = \dot{V}_{\text{air}} LWC = (\nu_{TS} A_{TS}) LWC$$

that depends on the liquid water content (LWC).

2.3. Droplet behaviour

A characteristic feature of an icing wind tunnel is the maximum diameter of droplets that can be tested in the icing wind tunnel. In order to determine this maximum diameter, the velocity and the temperature of the droplets must be calculated. The velocity of droplets can be calculated with the equation of motion

$$(5) m_d \frac{d\vec{u}}{dt} = -m_d \vec{g} + \frac{1}{2} \rho_{\text{air}} A_d c_D |\vec{u} - \vec{v}| (\vec{v} - \vec{u})$$

for a single droplet [17]. The water droplets in icing experiments can typically be treated as rigid spheres [17]. Therefore, the mass of the droplet becomes

$$(6) m_d = \frac{4}{3} \pi r_d^3 \rho_d,$$

the projected area of the droplet becomes

$$(7) A_d = \pi r_d^2,$$

and the drag coefficient can be calculated with the equation by Morrison [18]

$$(8) c_D = \frac{24}{Re} + \frac{2.6 \left(\frac{Re}{5.0} \right)^{1.52}}{1 + \left(\frac{Re}{5.0} \right)^{1.52}} + \frac{0.411 \left(\frac{Re}{2.63 \cdot 10^5} \right)^{-7.94}}{1 + \left(\frac{Re}{2.63 \cdot 10^5} \right)^{-8.00}} + \frac{0.25 \left(\frac{Re}{10^6} \right)}{1 + \left(\frac{Re}{10^6} \right)}$$

To solve equation (5), the derivatives can be transformed into differences. The gravity can be neglected as just the velocity in flow direction is calculated. By rearranging the terms, equation (5) can be reformulated as

$$(9) \Delta u = \frac{1}{2} \rho_{\text{air}} \frac{A_d}{m_d} c_D / \vec{u} \cdot \vec{v} / (\vec{v} \cdot \vec{u}) \Delta t.$$

Equation (9) can be solved by using a time-step procedure and using the velocity of the last time step for every term on the right-hand side.

The temperature of the droplets can be calculated by using the first law of thermodynamics [17]. The resulting heat balance

$$(10) \dot{E} = \dot{Q}_C + \dot{Q}_R$$

does not contain a term for the evaporative heat, because the relative humidity inside the icing wind tunnel can be assumed to be around 1. Instead, equation (10) contains the change of the internal energy of the droplet

$$(11) \dot{E} = \frac{4}{3} \pi r_d^3 \rho_d c_v \frac{dT_d}{dt}$$

on the left-hand side. The first term on the right-hand side is the rate of heat transfer due to convection

$$(12) \dot{Q}_C = 4 \pi r_d k (T_a - T_d) \frac{Nu}{2}$$

that depends on the Nusselt number Nu . The Nusselt number is a dimensionless parameter for the heat transfer. Because the droplets can be treated as rigid spheres, the correlation

$$(13) Nu = 2 + 0.6 Pr^{1/3} Re^{1/2}$$

is valid [19]. The second term on the right-hand side is the rate of heat transfer due to radiation

$$(14) \dot{Q}_R = 4 \pi r_d^2 \sigma \epsilon_d (T_a^4 - T_d^4).$$

As it was done with the equation of motion, equation (10) can be transformed by substituting the derivatives with differences. A rearrangement of the different terms leads to the following formulation:

$$(15) \Delta T_d = \frac{3(Q_C + Q_R)}{4 \pi r_d^3 \rho_d c_v} \Delta t.$$

This equation can be solved by using a time-step procedure and using the temperature of the last time step for the terms on the right-hand side.

Atmospheric icing depends on the diameter of the impinging droplets. Droplets in a natural cloud have a spectrum of droplet diameters. To describe the problem with one single parameter, a representative diameter is calculated. For icing experiments, the median volume diameter (MVD) is typically used for this purpose.

For the design of the icing wind tunnel, an MVD is specified. Since an MVD is representative of a spectrum of droplet sizes, a droplet diameter distribution has to be specified as well. The FAA Advisory Circular No 20-73A suggests using the Langmuir D distribution for the diameter distribution in an icing wind tunnel [20]. The largest droplets in the Langmuir D distribution have a diameter 2.22 times larger than the MVD.

3. RESULTS

Parameter	Value
maximum test section speed	35 m/s
maximum chord length	0.4 m
maximum angle of attack	8°
minimum air temperature	-15 °C
maximum LWC	3 g/m³
maximum MVD	40 µm

TAB 1: Requirements for the icing wind tunnel.

The requirements for the icing wind tunnel must be established before the design can be started. Since scaling is not feasible, real-life flight conditions need to be reproduced in the icing wind tunnel. This means that real UAV airfoils are tested in the icing wind tunnel at the same chord lengths and at the same airspeed as in the real flight. The consequent requirements are listed in TAB 1 and cover most in-cloud icing conditions, excluding supercooled large droplets (freezing rain/drizzle). Typical parameters for droplet clouds are listed in the certification guidelines by regulatory bodies such as EASA or FAA [21]. Because larger droplets and low temperatures increase the dimensions and the necessary power of the icing wind

tunnel, these values have to be limited. Earlier studies helped to identify the most relevant icing conditions, which was considered for the design specifications of this icing wind tunnel [22].

Another point that must be decided before the design process is, whether the icing wind tunnel shall be of the closed- or the open-return type. For this work, an open-return wind tunnel is favoured because it is smaller and typically cheaper than a comparable closed-return wind tunnel.

3.1. Wind tunnel design

The test section is designed with a height of 0.68 m to contain UAV airfoils without significant blockage effects in the test section. Additionally, the test section is designed with a width of 0.39 m. This was done to have a width of 0.3 m that is not affected by boundary layer effects. Measurements can be done on multiple spanwise locations on this chord section on account of the stochastic nature of the icing process.

The component upstream of the test section is the contraction nozzle. Higher area ratios of the contraction nozzle increase the flow quality, but also the overall size of the wind tunnel. Therefore, a medium contraction ratio of 9 was chosen. The nozzle contour influences the risk of separation and has a significant influence on the droplet size that can be tested in the wind tunnel. For the design of our icing wind tunnel, the AVA contour was selected. The AVA nozzle contour can be described by

$$(16) \frac{z(x)}{z_{TS}} = (\sqrt{AR} - 1) \left(1 - \frac{x}{L}\right)^3 \left[2 - \left(1 - \frac{x}{L}\right)^3\right] + 1.$$

The length of the nozzle must not be too short to prevent separation. According to Eckert et. al. [23], a nozzle length of more than 1.55 m is sufficient to prevent separation. Longer nozzles decrease the chance of separation even further. Additionally, longer nozzles decrease the final deviation between the droplet temperature and the target temperature as well as the final deviation between the droplet velocity and the target speed. Therefore, a slightly longer nozzle with a length of 1.74 m was selected.

A special feature of the designed icing wind tunnel is that the aspect ratio of the nozzle is changing over the nozzle length. This was done to have a square end at the beginning of the contraction despite the rectangular shape of the test section. A squared cross-section at the beginning is beneficial for the remaining components.

The settling area upstream of the contraction contains three components. Honeycombs and turbulence screens improve the flow quality. The third component, a spray system, is necessary to inject water droplets. Every component downstream of the spray system can collect water droplets and ice. Ice accumulations reduce the performance of every component and are therefore not wanted. Hence, the spray system must be placed downstream of the honeycombs and turbulence screens.

A large length-to-diameter ratio of the honeycombs leads to a better flow quality. Therefore, the designed honeycombs have a diameter of 0.01 m and a length of 0.08 m. A better flow quality can also be achieved by the usage of

turbulence screens with a low porosity. For this work, a porosity of 0.6 was chosen, because even lower values often lead to unsteady effects in the test section.

The problem of accumulating ice is also important for the position of the fan. Most open-return wind tunnels have a fan at the exit of the wind tunnel. In an icing wind tunnel, a fan at the exit would be subject to accumulate ice. This would reduce the performance significantly and therefore reduce the test capability of the icing wind tunnel. Hence, the fan must be placed at the inlet of the icing wind tunnel instead of the exit.

Not just the position of the fan needs to be decided, but also the type of fan. Three options were considered for this work. Centrifugal blowers are typically much larger in size than axial fans and therefore not beneficial for this work. Another option is to use multiple axial fans. The power needs for the fans in this matrix are lower compared to a single fan. This decreases the costs and also the size. There are however questions about the quality of the flow when multiple fans are used. Therefore, a single axial fan was chosen.

The selected axial fan is smaller in diameter than the settling area. Therefore, a diffuser is necessary to connect the two parts with each other. To keep the length of this diffuser short, a very high opening angle of 60° is chosen. Separation occurs in diffusers with such high opening angles, if no action is taken. The installation of two screens inside this wide-angle diffuser will prevent the flow from separation [24]. Because the settling area has a square cross-section and the axial fan a circular one, the wide-angle diffuser changes its cross-section over its length.

To have a good pressure recovery, a diffuser is placed downstream of the test section. This diffuser will have an opening angle of 3° and an area ratio of 2.5. These values are large and therefore favour the pressure recovery. The upstream end of the diffuser has the same rectangular cross-section as the test section. The separation risk depends on the opening angle of the diffuser. If the aspect ratio of the sides was kept the same over the length of the diffuser, the opening angle would be higher for the vertical side than for the horizontal and therefore the risk of separation would increase. Instead, a design with the opening angle of 3° for the vertical and horizontal side was chosen to decrease the risk of separation. Therefore, the aspect ratio changes over the length of the diffuser.

Overall, the designed icing wind tunnel has a length of about 8m and is 1.5 m x 1.5 m on its widest position. The wind tunnel in its completeness is shown in FIG 1.

According to equation (1), the volume flow through the icing wind tunnel will be $9.28 \text{ m}^3 \text{s}^{-1}$ for the airspeed formulated in TAB 1. This volume flow needs to be provided by the axial fan. Additionally, the fan must compensate all pressure losses that occur inside the icing wind tunnel. The total pressure loss is 339 Pa. A safety margin of 50% is recommended for the fan. Therefore, a fan with 500 Pa is necessary. A fan that is able to fulfil these requirements was selected during the design of this icing wind tunnel. This axial fan has a power need of 8.0 kW.

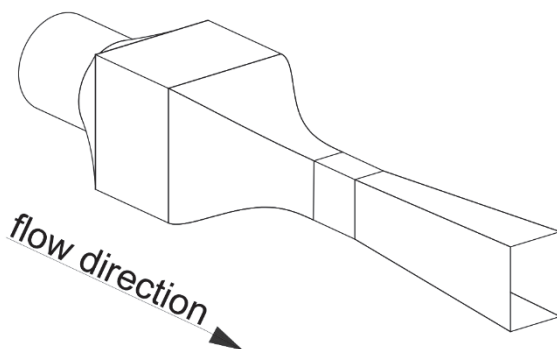


FIG 1: The final design of the icing wind tunnel.

The design done until this point was the design of a conventional wind tunnel that fits a UAV airfoil in the test section and has no separation according to the presented rules. To use the wind tunnel as an icing wind tunnel, a suitable spray system needs to be selected as well as a suitable cooling unit.

3.2. Droplet behaviour

The design or selection of a suitable spray system is a large topic itself and was therefore not included in this work. The behaviour of droplets between the spray system and the test object can be checked nevertheless. By using equation (9), the development of the velocity of droplets with different diameters can be calculated. Droplets with larger diameters adjust more slowly to the higher airspeed. Therefore, the final deviation between the droplet velocity and the airspeed is larger for droplets with larger diameters, as visualized in FIG 2.

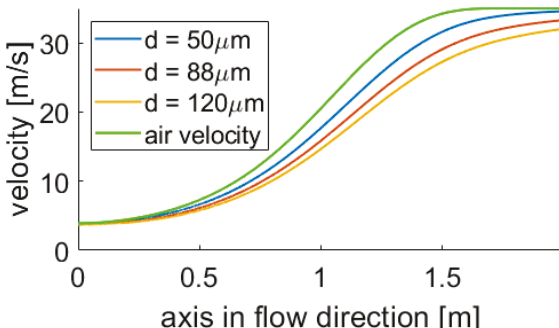


FIG 2: Development of the velocity of droplets with different diameters.

The development of the temperature of the droplets can be calculated with equation (15). As it is the case for the velocity, also the temperature of larger droplets adjusts more slowly to the temperature of the air. Hence, also the final temperature deviation is larger for droplets with a larger diameter as FIG 3 shows.

If the droplet does not cool down close enough to the target temperature, the process of ice accumulation can be different in the icing wind tunnel test than it would be in a real-life case with the same ambient conditions. The same is true if the final velocity deviation is too large. Therefore,

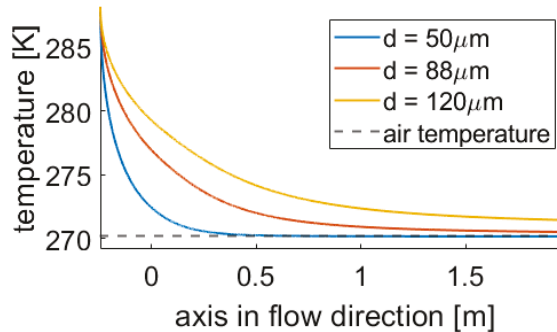


FIG 3: Development of the temperature of droplets with different diameters.

the final deviations for both the velocity and the temperature must be small to have good comparability of the icing wind tunnel tests with situations in the real flight. This is why limits need to be formulated for the acceptable deviations. From the experience with prior wind tunnel tests, the droplet temperature must not deviate more than 0.5°C if the air temperature is -3°C and the final velocity deviation must be at most 2 m/s for the worst case. The calculations shown in FIG 2 and FIG 3 result in a maximum diameter of around 88 μm that can be tested inside the designed icing wind tunnel without violating the formulated deviation limits. According to the Langmuir D distribution for the droplet diameters, this means that the maximum possible MVD in the icing wind tunnel is 40 μm .

While an MVD of 40 μm is sufficient according to the requirements formulated in TAB 1, it is not enough to test the whole range of icing conditions in the certification requirements. If larger diameters shall be tested in an icing wind tunnel as well, the contraction nozzle must be longer as shown in FIG 4. For small diameters, the distance between the spray system and the nozzle beginning and the distance between the test section beginning and the test object is already long enough to achieve satisfying adaption. Therefore, a contraction nozzle would not be necessary for the droplets. However, if the nozzle is too short, the flow will separate. Hence, the nozzle length cannot be shortened too much.

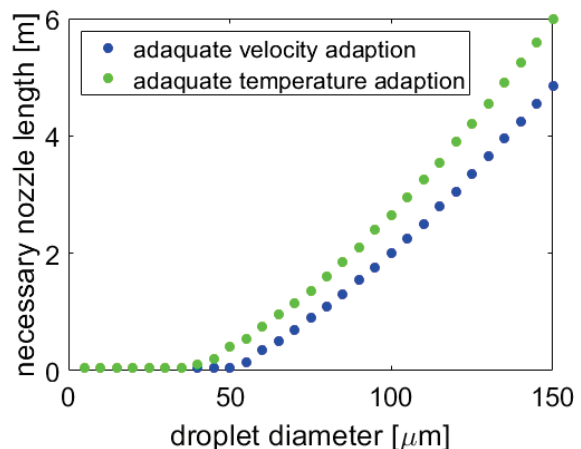


FIG 4: Necessary length of the contraction nozzle to fulfil the requirements.

3.3. Cooling power

The fan power has to be considered for the cooling requirements as well as the latent heat and the sensible heat. The latter two depend on the LWC. This is because higher LWCs mean more water in the icing wind tunnel that needs to be cooled and that can freeze. FIG 5 shows the produced heat in dependence of the LWC for an air temperature of -10 °C. The resulting maximum cooling power is therefore around 20.5 kW.

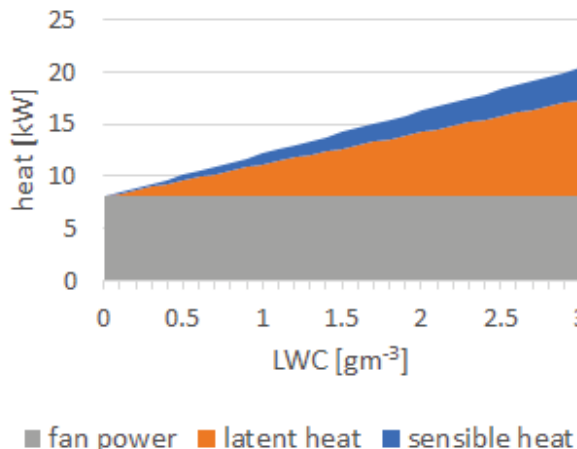


FIG 5: Produced heat in dependence of the LWC.

3.4. CFD simulations

The flow field in the icing wind tunnel was investigated with a CFD simulation. The simulation was done in 3D with the software ANSYS FENSAP-ICE. The grid contains the settling area, the contraction nozzle, the test section, and the diffuser, but no internal structures like a test object. The icing wind tunnel was designed according to rules and equations to prevent flow separation in any part. However, the CFD simulation shows flow separation in the corner of the icing wind tunnel over almost the whole length as can be seen in FIG 6.



FIG 6: CFD simulation of the area of flow separation.

If the flow separates as it does in FIG 6, the flow quality in the test section suffers. Therefore, also the quality of the results of the experiments done in the icing wind tunnel would decrease.

Not only the flow quality is potentially suffering, but also the pressure losses might increase. The pressure loss over the components of the CFD simulation is about 220 Pa. The pressure loss for the same components calculated with equations by [15] and [23] is just 73 Pa. Hence, the pressure loss calculated with the CFD simulation is about three times higher than the originally calculated pressure loss.

4. DISCUSSION

The results, especially FIG 2 and FIG 3, show that the designed icing wind tunnel is capable to fulfil the requirements formulated in TAB 1 for an icing wind tunnel for UAVs. Therefore, the presented design offers an excellent base for a further and more in-depth design of an icing wind tunnel. Building such an icing wind tunnel would offer a much-needed facility to do tests on the effects of atmospheric icing on UAVs and to test ice protection systems under realistic conditions.

However, there are more steps needed before an icing wind tunnel can really be used. This work states calculated power needs for the fan and the cooling unit and therefore offers a first guess for those components. The final selection of suitable options is however still open. Especially the cooling unit offers multiple options, e. g. placing the designed icing wind tunnel in a climate chamber or injecting liquid nitrogen to cool the air.

Another topic that still needs more consideration is the spray system. This is a very important topic that was not covered in this work. A suitable spray system must be able to inject droplets with the chosen MVD and LWC and the droplets must spread enough to cover the whole test section.

Additionally, the CFD results show that the designed icing wind tunnel has shortcomings that were not covered by the rules and equations that were used to design the wind tunnel. Therefore, a further analysis of the CFD results and a following change of the design is necessary as well.

5. SUMMARY

This paper presents the design of an icing wind tunnel that is specially designed for medium-sized fixed-wing UAVs. The icing wind tunnel has a test section size of 0.68 m x 0.39 m. The overall dimensions of the wind tunnel are 8 m length and 1.5 m x 1.5 m in width and height.

Calculations of the development of the temperature and the velocity of droplets in the designed icing wind tunnel were done. The results show that droplet MVDs of 40 µm and less can be tested in the designed icing wind tunnel. This covers the largest and more severe part of the icing conditions.

Additionally, the necessary power to run the wind tunnel is calculated. A suitable fan needs to have a power of around 8 kW. To cool the icing wind tunnel and ensure a steady run, a cooling unit needs to remove about 20 kW.

The paper also presents the results of CFD calculations of the flow field in the designed icing wind tunnel. The results show that the flow is probable to separate and therefore reduce the flow quality and increase the pressure loss in the wind tunnel.

6. ACKNOWLEDGEMENTS

This project received funding from the Research Council of Norway under grant number 223254 and 296228. CFD simulations were conducted on the Vilje supercomputer,

Notur/NorStore project code NN9613K.

This work was part of a Master's thesis of J. Wallisch. The authors thank the European Union for the financial support via the Erasmus program. Additionally, the authors thank Prof. Dr. Weigand from the Institute of Aerospace Thermodynamics of the University of Stuttgart for the co-supervision of the Master's thesis.

7. REFERENCES

- [1] Bragg, M.B., Broeren, A.P., and Blumenthal, L.A., "Iced-Airfoil Aerodynamics", *Prog. Aerosp. Sci.* 41(5), pp. 323-362, 2005.
- [2] Peck, L., Ryerson, C.C., and Martel, C.J., "Army Aircraft Icing," US Army Corps of Engineers - Cold Regions Research and Engineering Laboratory Technical Report ERDC/CRREL TR-02-13, 2002.
- [3] Hann, R. and Johansen, T. A., "Unsettled Topics in Unmanned Aerial Vehicle Icing," SAE EDGE Research Report EPR2020008, SAE International, 2020.
- [4] Szilder, K. and McIlwain, S., "In-Flight Icing of UAVs – The Influence of Reynolds Number on the Ice Accretion Process," SAE Technical Paper 2011-01-2572, 2011.
- [5] Hann, R., "Atmospheric Ice Accretions, Aerodynamic Icing Penalties, and Ice Protection Systems on Unmanned Aerial Vehicles," PhD thesis, Norwegian University of Science and Technology, 2020.
- [6] IEA Wind Task 19, "Available Technologies for Wind Energy in Cold Climates," Technical report, 2018.
- [7] Koenig, G.G., Ryerson, C.C., and Kmiec, R., "UAV Icing Flight Simulation," in *40th Aerospace Sciences Meeting & Exhibit*, Reno, 2002, AIAA-2002-0812.
- [8] Tran, P., Baruzzi, G., Tremblay, F., Benquet, P. et al., "FENSAP-ICE Applications to Unmanned Aerial Vehicles (UAV)," in *42nd AIAA Aerospace Sciences Meeting and Exhibit*, pp. 390-402, 2004.
- [9] Szilder, K. and Yuan, W., "In-Flight Icing on Unmanned Aerial Vehicle and its Aerodynamic Penalties," *Prog. Flight Phys.* 9, pp. 173-188, 2017.
- [10] Hann, R., "UAV Icing: Comparison of LEWICE and FENSAP-ICE for Ice Accretion and Performance Degradation," in *2018 Atmospheric and Space Environments Conference*, AIAA Aviation, Atlanta, ISBN 978-1-62410-558-6, 2018.
- [11] Hann, R., Borup, K., Zolich, A., Sorensen, K. et al., "Experimental Investigations of an Icing Protection System for UAVs," SAE Technical Paper 2019-01-2038, 2019.
- [12] Hann, R., "UAV Icing: Ice Accretion Experiments and Validation," SAE Technical Paper 2019-01-2037, 2019.
- [13] Kind, R., Potapczuk, M., Feo, A., Golia, C., and Shah, A., "Experimental and computational simulation of in-flight icing phenomena," *Prog. Aerosp. Sci.* 34(5), pp. 257-345, 1998.
- [14] Wallisch, J., "Design of an Icing Wind Tunnel for UAVs", Master's thesis, University of Stuttgart and Norwegian University of Science and Technology, 2020.
- [15] Barlow, J., Rae, W., and Pope, A., "Low-Speed Wind Tunnel Testing," Wiley, 1999. ISBN 9780471557746.
- [16] Bansmer, S., Baumert, A., Sattler, S., Knop, I., Leroy, D., Schwarzenboeck, A., Jurkat-Witschas, T., Voigt, C., Pervier, H., and Esposito, B., "Design, Construction and Commissioning of the Braunschweig Icing Wind Tunnel," *Atmospheric Measurement Techniques Discussions* 11(6), pp. 3221-3249, 2018.
- [17] Gates, E., Lam, W., and Lozowski, E., "Spray evolution in icing wind tunnels". *Cold Regions Science and Technology* 15(1), pp. 65-74, 1988.
- [18] Morrison, F. A., "Data Correlation for Drag Coefficient for Sphere," Department of Chemical Engineering, Michigan Technological University, 2016.
- [19] Knudsen, J. G. and Katz, D. L. V., "Fluid dynamics and heat transfer," Huntington, N.Y., R. E. Krieger Pub. Co, 1979. ISBN 978-0-88275-917-3.
- [20] Federal Aviation Administration (FAA), "Aircraft Icing Protection," Advisory Circular No 20-73A, 2006.
- [21] European Aviation Safety Agency, "Certification Specifications and Acceptable Means of Compliance for Large Aeroplanes CS-25", chapter Appendix C. 2016.
- [22] Fajt, N., Hann, R., and Lutz, T., "The Influence of Meteorological Conditions on the Icing Performance Penalties on a UAV Airfoil," In *8th European Conference for Aeronautics and Aerospace Sciences (EUCASS)*, 2019.
- [23] Eckert, W., Mort, K., and Jope, J., "Aerodynamic design guidelines and computer program for estimation of subsonic wind tunnel performance," Technical note TN D-8243, NASA, 1976.
- [24] Mehta, R. and Bradshaw, P., "Design rules for small low speed wind tunnels," *The Aeronautical Journal* 83(827), pp. 443-453, 1979.